

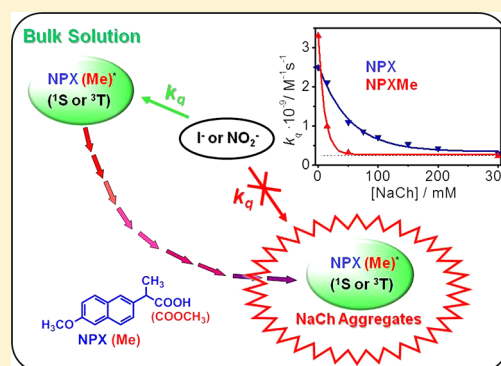
Photophysical Probes To Assess the Potential of Cholic Acid Aggregates as Drug Carriers

Miguel Gomez-Mendoza, Edurne Nuin, Inmaculada Andreu, M. Luisa Marin, and Miguel A. Miranda*

Instituto Universitario Mixto de Tecnología Química (UPV-CSIC), Universitat Politècnica de València, Avenida de los Naranjos s/n, 46022 Valencia, Spain

S Supporting Information

ABSTRACT: The two enantiomers of the nonsteroidal antiinflammatory drug naproxen and of its methyl ester have been selected as representative probes with markedly different hydrophobicity to assess the potential of cholic acid aggregates as drug carriers by means of photophysical techniques. The different distribution of the probes between bulk solution and aggregates has been assessed by quenching of their singlet and triplet excited states by iodide and nitrite anions, respectively. This straightforward photophysical methodology can, in principle, be extended to a variety of drugs containing a photoactive chromophore.



INTRODUCTION

Bile acids are a family of natural amphiphilic steroids biosynthesized in the liver.^{1,2} Their concave α -face shows hydrophilic character, whereas their β -face is more hydrophobic. These properties result in the formation of aggregates in solution. Thus, at low concentrations, the interaction of bile salts by their hydrophobic β -faces leads to formation of primary aggregates, whereas at higher bile salt concentrations, further association between the primary aggregates gives rise to the secondary ones, in which in addition to hydrophobic sites, hydrophilic microenvironments can be found (Chart 1).³ Among their physiological functions, bile acid aggregates play an important role in the solubilization of lipids.¹ For this reason, they could, in principle, be used as carriers in the pharmaceutical application of poorly soluble drugs, extending their transport through the intestinal epithelium; however, very few examples of this concept have been reported: for instance, solubilization of β -blockers,^{4,5} benzodiazepines^{5,6} or morphine.⁷

The drug–carrier interaction has been studied by different techniques, including microcalorimetry,⁴ spectrophotometry,⁶ ESR,⁵ or saturation transfer difference (STD) NMR experiments.⁷ Some of them are based on indirect measurements that make use of extra probes capable of inducing additional interactions, and others do not inform on the accessibility of the drugs inside the aggregates. Moreover, high drug concentrations may be required because of the low sensitivity of the employed techniques, thus limiting their applicability to highly hydrophilic compounds. Therefore, direct, reliable, and sensitive methodologies are still needed to study the interactions between drugs and bile salt aggregates. In this context, photophysical techniques, such as fluorescence or laser flash photolysis, have proven potential to investigate the

binding of different model guests (e.g., naphthalene derivatives) to cholic acid aggregates⁸ and provide information on the accessibility of guests' excited states to water-soluble quenchers.^{9,10} In addition, we have recently made use of the singlet excited state of probe molecules as a reporter to build up speciation diagrams for the different types of cholic acid aggregates (the most abundant bile acid in humans)¹¹ or as a sensitive tool to investigate stereodifferentiation in the quenching of different tryptophan derivatives inside the aggregates.¹²

Naproxen (NPX) is widely used as a safe, tolerable, and highly effective nonsteroidal antiinflammatory drug. Because it contains a naphthalene chromophore, this drug is, in principle, a suitable probe that can be studied by means of photophysical techniques.^{13–18}

With this background, the goal of the present work is to use the free carboxylic acid and the methyl ester derivatives of naproxen in their two enantiomeric forms, (R)- or (S)-NPX and (R)- or (S)-NPXMe, as probes with markedly different hydrophilicity to assess the potential of sodium cholate (NaCh) aggregates as drug carriers by means of photophysical techniques (Chart 1). Quenching of the singlet and triplet excited states of NPX(Me) by NaI and NaNO₂, acting from the aqueous phase, has been investigated by means of steady-state and time-resolved fluorescence spectroscopy and also by laser flash photolysis. The obtained quenching constant values provide evidence for the extensive incorporation of the drugs

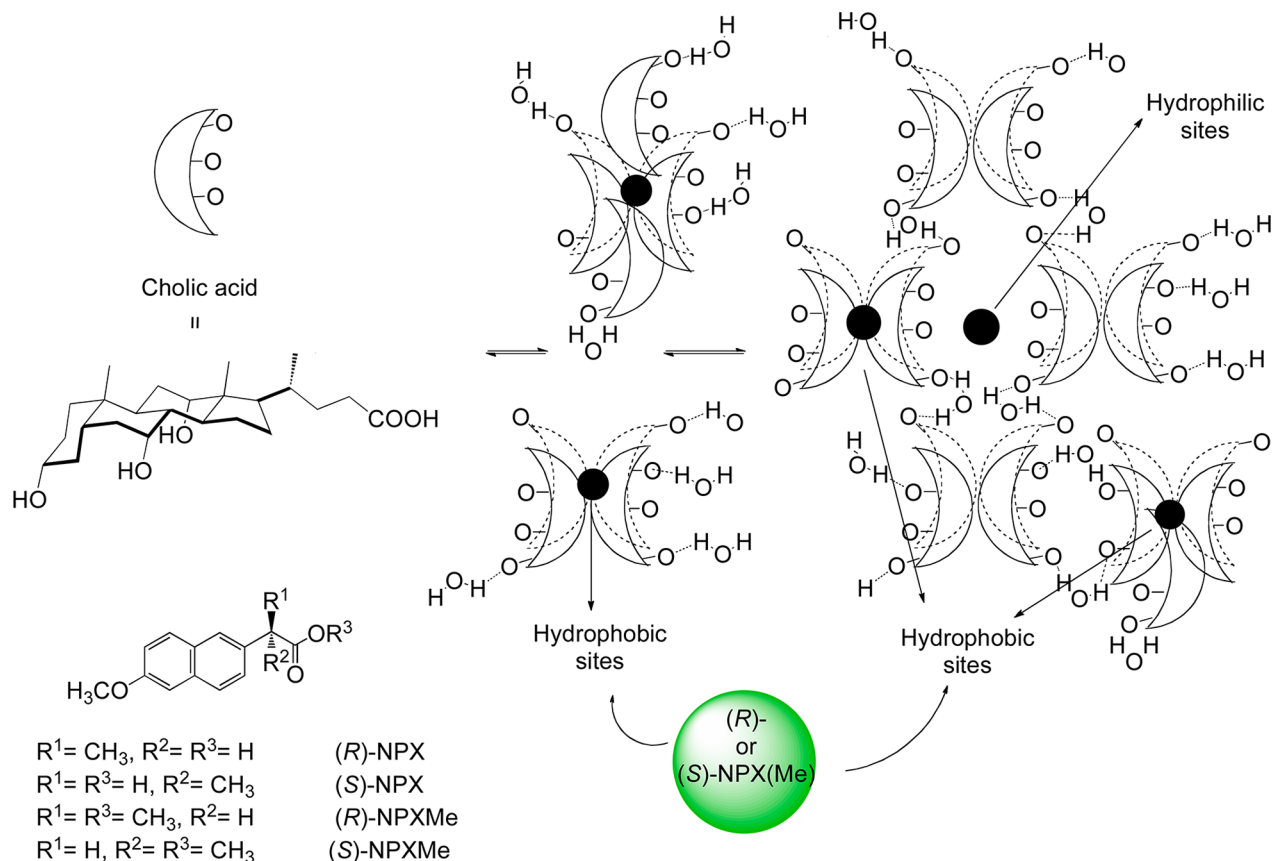
Received: May 15, 2012

Revised: August 9, 2012

Published: August 11, 2012



Chart 1. Representation of Naproxen Derivatives (R)- or (S)-NPX(Me) Incorporated into Cholic Acid Aggregates



into the hydrophobic binding sites of the aggregates if the appropriate concentration of bile acid is chosen.

EXPERIMENTAL METHODS

Chemicals. Sodium cholate (NaCh), (R)- and (S)-NPX, dimethylsulfoxide (DMSO), and NaCl with purity higher than 99% were purchased from Sigma-Aldrich (Steinheim, Germany) and were used without further purification. The methyl esters (R)- and (S)-NPXMe were synthesized as previously reported.¹⁹

Instrumentation. Absorption spectra were recorded on a Cary 300 UV–vis spectrophotometer (UV0811M209, Varian). Fluorescence spectra were obtained with a LP S-220B (Photon Technology International) equipped with a 75 W Xe lamp and were corrected with baseline control experiments to subtract the solvent Raman emission. Fluorescence lifetime measurements were based on a PTI (TM-2/2003) equipped with a H₂/N₂ (50/50, 1.5 ns pulse width) lamp and a stroboscopic detector. The laser flash photolysis (LFP) studies were carried out with a pulsed Nd:YAG LS2137 V LOTIS TII at the excitation wavelength of 266 nm. The single pulses were ~10 ns in duration, and the energy was lower than 20 mJ/pulse. The laser flash photolysis system consisted of the pulsed laser, a 77250 Oriol monochromator, and an oscilloscope DP04054 Tektronix. All the output signal from the oscilloscope was transferred to a personal computer.

Preparation of Sodium Cholate Aggregates. Solutions of NaCh at different concentrations were freshly obtained by dissolving the appropriate amount of the salt in 0.2 M NaCl. The concentration of NPX(Me) in the presence of NaCh was 60 μM , obtained from 5 mM DMSO stock solutions.

Quenching Experiments. The absorbance of the solutions for the fluorescence experiments was kept below 0.1 at the excitation wavelength ($\lambda_{\text{exc}} = 316 \text{ nm}$). In a typical quenching experiment, the appropriate volumes of a freshly prepared NaI solution (2 M) were added to the NPX(Me) aerated solutions with the corresponding concentration of NaCh. For the LFP quenching experiments, the absorbance of the solutions was kept at ~0.3 at $\lambda_{\text{exc}} = 266 \text{ nm}$. In a typical quenching experiment, the appropriate volumes of a freshly prepared NaNO₂ solution (250 mM) were added to the purged NPX(Me) solutions with the corresponding NaCh concentration. All the photophysical measurements were performed at room temperature in a quartz cell of 1.0 cm optical path length.

RESULTS AND DISCUSSION

The UV–vis spectra of (R)- or (S)-NPX and (R)- or (S)-NPXMe were recorded in 0.2 M aqueous NaCl in the presence of different concentrations of NaCh (up to 300 mM). The shape and position of the absorption bands were all coincident, with maxima at 262, 271, 316, and 332 nm. The emission spectra, both in solution and in the presence of the aggregates, showed a maximum at ~355 nm at $\lambda_{\text{exc}} = 316 \text{ nm}$ (Figures S1 and S2 of the Supporting Information). Fluorescence quantum yields (ϕ_F) were determined in air-equilibrated solutions, in the presence and in the absence of the aggregates, using (S)-NPX in deaerated acetonitrile as standard ($\phi_F = 0.47$).²⁰ Only a small increase in the ϕ_F values was observed upon incorporation into the aggregates (from 0.39 to 0.41). Likewise, the lifetimes of the singlet excited states (τ_s) increased from 10 ns in aqueous solution to 12 or 15 ns for NPX or NPXMe, respectively, within the aggregates. Therefore, these differences were not

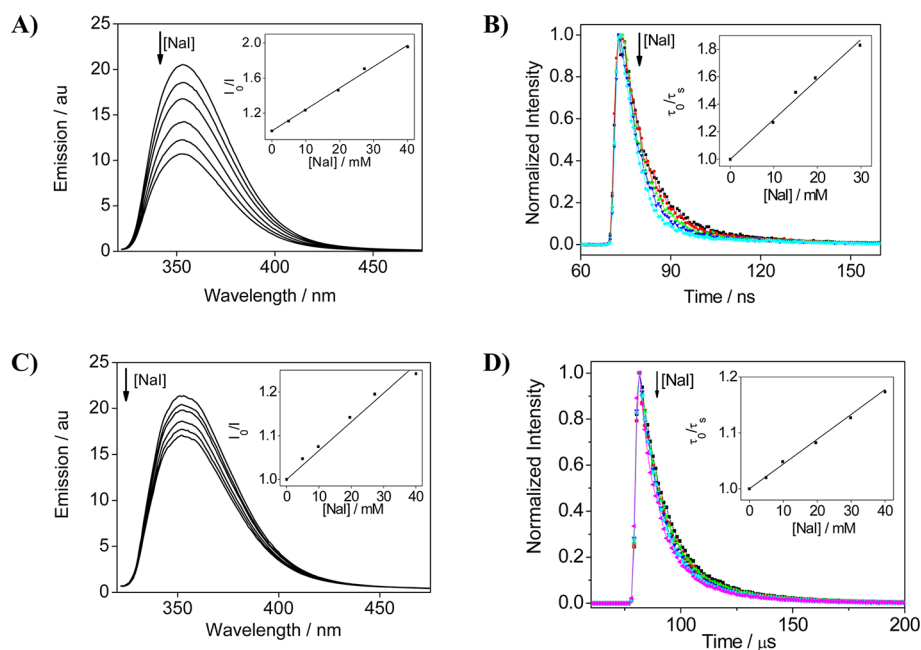


Figure 1. Changes in the emission spectra or emission decay traces of (*R*)-NPX upon addition of increasing concentrations of NaI recorded in 0.2 M aqueous NaCl at different NaCh concentrations: (A and B) 0 mM and (C and D) 200 mM. Insets: corresponding Stern–Volmer plots.

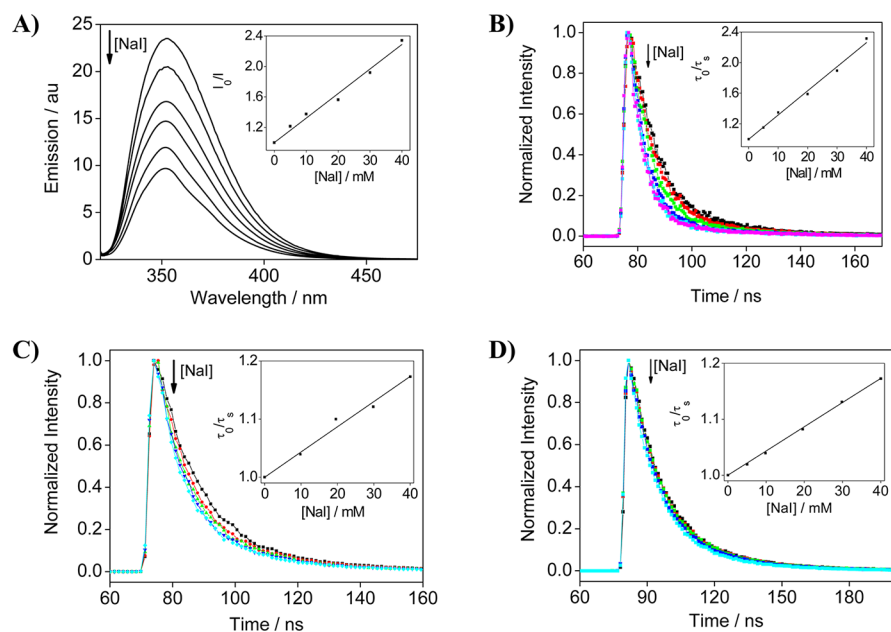


Figure 2. Changes in the emission spectra or emission decay traces of (*R*)-NPXMe upon addition of increasing concentrations of NaI recorded in 0.2 M aqueous NaCl at different NaCh concentrations: (A and B) 2 mM, (C) 50 mM, and (D) 200 mM. Insets: corresponding Stern–Volmer plots.

large enough to evaluate the incorporation of NPX(Me) into the hydrophobic sites of the primary/secondary aggregates in a reliable way.

To investigate the extent of binding (at NaCh concentrations up to 300 mM), quenching experiments using an ionic salt (NaI) that mainly remains in water were performed by means of steady-state and time-resolved emission spectroscopy. The dynamic quenching efficiency can be interpreted as a measure of the probe accessibility to the quencher.⁸

In fact, the emission of NPX was quenched by increasing concentrations of iodide with no changes in the position of the maxima. Figure 1A and C shows the fluorescence spectra for the case of (*R*)-NPX, as a representative example, upon

addition of increasing concentrations of NaI and recorded in 0.2 M aqueous solution of NaCl and in the presence of 200 mM NaCh, respectively. The corresponding changes in the emission decay traces are shown in Figure 1B and D, indicating that the quenching is, indeed, dynamic. A gradual decrease in the quenching rate constants was observed from solution to 300 mM NaCh for both enantiomers. Parallel experiments were performed on the corresponding methyl esters (Figures 2A–D); again, dynamic quenching by iodide was observed (see Figures S3–S10 and Table 1, Supporting Information).

Overall, the extent of emission quenching by iodide decreased with increasing affinity of the drug to the hydrophobic sites of the aggregates. Interestingly, when the

apparent quenching rate constants (k_q^S) were plotted against NaCh concentration, a sharp decrease was found for the methyl esters NPXMe, whereas a much more gradual decrease was observed for the free carboxylic acids NPX (Figure 3). Thus, a

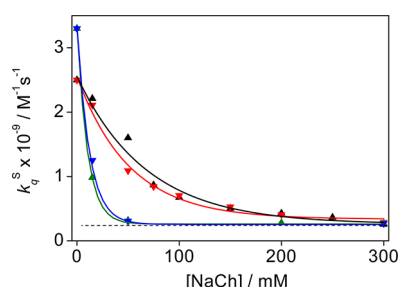


Figure 3. Plot of the fluorescence quenching rate constants (k_q^S $M^{-1} s^{-1}$) by iodide for (R)-NPX (\blacktriangle), (S)-NPX (red inverted triangle), (R)-NPXMe (green triangle), and (S)-NPXMe (blue inverted triangle) versus concentration of NaCh in aerated 0.2 M aqueous NaCl solutions.

very efficient quenching occurred for NPX(Me) at 2 mM NaCh ($3.3 \times 10^9 M^{-1} s^{-1}$), whereas in the presence of 50 mM NaCh, this value dropped to $2.9\text{--}3.2 \times 10^8 M^{-1} s^{-1}$, indicating that NPXMe is mainly incorporated into the hydrophobic sites of the aggregates at this concentration. In the case of (R)- or (S)-NPX, the quenching constant values varied from $2.4 \times 10^9 M^{-1} s^{-1}$ in solution to $2.6\text{--}2.9 \times 10^8 M^{-1} s^{-1}$ at 300 mM NaCh. A decrease in the quenching constant of 1 order of magnitude has already been observed in the literature for fluorescent probes such as naphthalene or pyrene.⁹ Taking into account that at $[NaCh] \geq 50$ mM, more than 95% of cholic acid is forming secondary aggregates,¹¹ the observed trends for the acids and their methyl esters can be interpreted on the basis of their different partition between the bulk solution and the hydrophobic sites of the hosts provided by the primary/secondary aggregates.

In a different, yet complementary approach, laser flash photolysis experiments were performed on NPX(Me) in solution and at different NaCh concentrations, up to 200 mM (see Figure 4 for the case of (S)-NPX as a representative example). The transient absorption spectra within the aggregates displayed the main band at 440 nm, characteristic of the triplet–triplet absorption in solution (Figure 4A).²¹ Interestingly, a significant increase in the triplet lifetime was observed at high NaCh concentration, which was associated with the incorporation of the drug into the aggregates (Figure

4B). In all cases, the decays of the triplet guests in the presence and the absence of bile salts were fitted to a monoexponential function.

When the triplet lifetimes were measured in the presence of NaNO₂, a clear quenching was observed, in agreement with the results obtained with time-resolved fluorescence. Again, the apparent rate constants for triplet quenching (k_q^T) by nitrite reflected not only the actual quenching constant but also the percentage of NPX(Me) remaining in solution. They were strongly dependent on the concentration of NaCh, ranging from $1.5 \times 10^9 M^{-1} s^{-1}$ for (R)- or (S)-NPX in solution and $2.3 \times 10^9 M^{-1} s^{-1}$ for (R)- or (S)-NPXMe at 2 mM NaCh to $\sim 2.0 \times 10^8 M^{-1} s^{-1}$ for the corresponding values within the hydrophobic sites of the aggregates (Figure 5). In general, quenching plots were linear; however, at 15 mM NaCh concentration, Stern–Volmer plots for (R)- or (S)-NPXMe were curved. This can be attributed to the mobility of the triplet excited state of the guest between the host and the bulk aqueous phase, and therefore, data were analyzed by means of the previously reported model.^{8,22} Thus, the k_q^T values obtained by applying this model were slightly lower ($2.0 \times 10^8 M^{-1} s^{-1}$ and $1.9 \times 10^8 M^{-1} s^{-1}$ for (S)-NPXMe and (R)-NPXMe, respectively) than those determined directly by the Stern–Volmer relationships (Table 2, Supporting Information). Interestingly, the curved plots were found only for the more hydrophobic guest at intermediate NaCh concentrations, where comparable amounts of free and bound guest coexist.

In accordance with the results obtained for quenching of the singlet excited state, a sharper decrease in the k_q^T values was observed for the more hydrophobic NPXMe with increasing NaCh concentration until reaching a plateau ($[NaCh] \sim 50$ mM) (Figure 6). This indicates a high affinity to the protected hydrophobic environments provided by the aggregates. Conversely, the k_q^T decrease for NPX was more gradual, as anticipated from the higher hydrophilic character of the free acid, which results in a less efficient protection by the aggregates.

CONCLUSIONS

In conclusion, photophysical techniques have been demonstrated to be direct, sensitive, and straightforward methodologies to assess the potential of bile acid aggregates as drug carriers. This concept has been proven using (R)- or (S)-NPX and (R)- or (S)-NPXMe as representative probes with different hydrophobicities and can, in principle, be extended to other drugs containing photoactive chromophores. Quenching of singlet and triplet excited states using ionic salts mainly residing

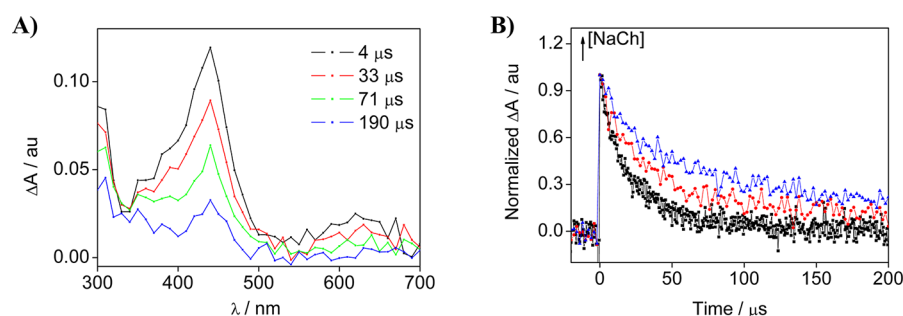


Figure 4. (A) Transient absorption spectra for (S)-NPX after laser flash excitation ($\lambda_{exc} = 266$ nm), obtained in deaerated aqueous 0.2 M NaCl solution of 200 mM NaCh. (B) Normalized decay traces monitored at 420 nm in the presence of different NaCh concentrations: (\blacksquare) 0, (red dot) 100, (blue triangle) 200 mM.

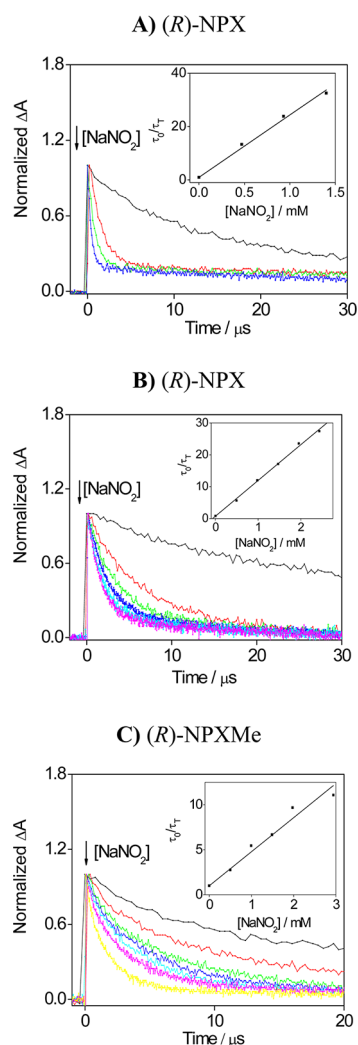


Figure 5. Changes in the triplet lifetime of (R)-NPX(Me) in deaerated 0.2 M aqueous NaCl, recorded at 440 nm, upon addition of increasing amounts of NaNO₂ at different NaCh concentrations: (A) 0 mM and (B and C) 200 mM. Insets: corresponding Stern–Volmer plots. In all cases, the triplet decays were fitted to a monoexponential function, with R^2 values higher than 0.98.

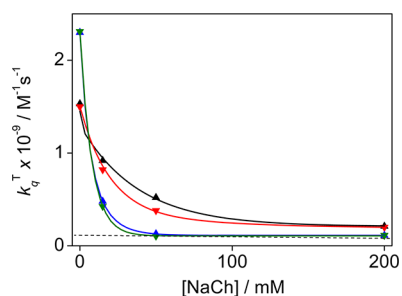


Figure 6. Plot of the triplet quenching rate constants (k_q^T , $M^{-1} s^{-1}$) by sodium nitrite for (R)-NPX (▲), (S)-NPX (red inverted triangle), (R)-NPXMe (blue triangle), and (S)-NPXMe (green inverted triangle) versus increasing concentrations of NaCh in deaerated 0.2 M aqueous NaCl solutions.

in the aqueous phase has provided evidence for the different distribution of the free carboxylic acids and their esters between the bulk solution and the aggregates. Interestingly, it has been demonstrated that even hydrophilic drugs can be substantially

incorporated into the aggregates if the appropriate concentrations of bile salts are chosen. Current work is directed at investigating whether the NaCh based systems, in addition to being appropriate as drug carriers, may be developed into drug delivery systems, which requires controlled release of the active compounds at the specific targets responsible for the pharmacological action.

■ ASSOCIATED CONTENT

Supporting Information

Figure S1: absorption spectra. Figures S2–S10: emission spectra and results of quenching experiments. Figures S11–S14: results of triplet quenching experiments. Tables 1 and 2: rate constants for singlet and triplet quenching by iodide and nitrite, respectively. This material is available free of charge via the Internet at <http://pubs.acs.org>.

■ AUTHOR INFORMATION

Corresponding Author

*Fax: (+34)963879444. E-mail: mmiranda@qim.upv.es.

Notes

The authors declare no competing financial interest.

■ ACKNOWLEDGMENTS

We gratefully acknowledge financial support from the Generalitat Valenciana (GV/2009/104 and Prometeo Program 2008/090), the Spanish Government (Red RETICS de Investigación de Reacciones Adversas a Alergenos y Fármacos (RIRAAF)), CTQ2009-13699 and Predoctoral FPU fellowship AP2008-03295 for M. G.-M.).

■ REFERENCES

- (1) Hofmann, A. F. *Arch. Intern. Med.* **1999**, *159*, 2647–2658.
- (2) Hofmann, A. F.; Hagey, L. R. *Cell. Mol. Life Sci.* **2008**, *65*, 2461–2483.
- (3) Small, D. M.; Penkett, S. A.; Chapman, D. *Biochim. Biophys. Acta* **1969**, *176*, 178–189.
- (4) Grosvenor, M. P.; Lofroth, J. E. *Pharm. Res.* **1995**, *12*, 682–686.
- (5) Reis, S.; Moutinho, C. G.; Pereira, E.; de Castro, B.; Gameiro, P.; Lima, J. J. *Pharm. Biomed. Anal.* **2007**, *45*, 62–69.
- (6) de Castro, B.; Gameiro, P.; Guimaraes, C.; Lima, J.; Reis, S. J. *Pharm. Biomed. Anal.* **2001**, *24*, 595–602.
- (7) Posa, M.; Csanadi, J.; Kover, K. E.; Guzsvany, V.; Batta, G. *Colloids Surf. B* **2012**, *94*, 317–323.
- (8) Rinco, O.; Nolet, M. C.; Ovans, R.; Bohne, C. *Photochem. Photobiol. Sci.* **2003**, *2*, 1140–1151.
- (9) Ju, C.; Bohne, C. *Photochem. Photobiol.* **1996**, *63*, 60–67.
- (10) Ju, C.; Bohne, C. *J. Phys. Chem.* **1996**, *100*, 3847–3854.
- (11) Gomez-Mendoza, M.; Marin, M. L.; Miranda, M. A. *J. Phys. Chem. Lett.* **2011**, *2*, 782–785.
- (12) Cuquerella, M. C.; Rohacova, J.; Marin, M. L.; Miranda, M. A. *Chem. Commun.* **2010**, *46*, 4965–4967.
- (13) Jimenez, M. C.; Miranda, M. A.; Tormos, R. J. *Photochem. Photobiol., A* **1997**, *104*, 119–121.
- (14) Perez-Ruiz, R.; Alonso, R.; Nuin, E.; Andreu, I.; Jimenez, M. C.; Miranda, M. A. *J. Phys. Chem. B* **2011**, *115*, 4460–4468.
- (15) Vaya, I.; Perez-Ruiz, R.; Lhiaubet-Vallet, V.; Jimenez, M. C.; Miranda, M. A. *Chem. Phys. Lett.* **2010**, *486*, 147–153.
- (16) Nuin, E.; Andreu, I.; Torres, M. J.; Jimenez, M. C.; Miranda, M. A. *J. Phys. Chem. B* **2011**, *115*, 1158–1164.
- (17) Costanzo, L. L.; De Guidi, G.; Condorelli, G.; Cambria, A.; Fama, M. J. *Photochem. Photobiol., B* **1989**, *3*, 223–235.
- (18) Partyka, M.; Au, B. H.; Evans, C. H. *J. Photochem. Photobiol., A* **2001**, *140*, 67–74.

- (19) Tsai, S. W.; Huang, C. M. *Enzyme Microb. Technol.* **1999**, *25*, 682–688.
- (20) Murov, S. L. C., I.; Hug, G. L. *Handbook of Photochemistry*; 2nd ed.; Marcel Dekker: New York, 1993.
- (21) Bosca, F.; Marin, M. L.; Miranda, M. A. *Photochem. Photobiol.* **2001**, *74*, 637–655.
- (22) Pace, T. C. S.; Bohne, C. Application of Photophysics to the Study of Supramolecular Dynamics. In *CRC Handbook of Organic Photochemistry and Photobiology*, 3rd ed.; Griesbeck, A., Oelgemöller, M., Ghetti, F., Eds.; CRC Press: Boca Raton, 2012; Vol. 2, pp 981–1001.